

An Analytical Observation of Soret Effects and Double Diffusive Convection in between Vertical Plates

Hadiza Nass Sani



Institute of Education, Ahmadu Bello University, Zaria, Nigeria

*Corresponding author's email: hadizanass@yahoo.com

ABSTRACT

The Soret effect in fluids is a thermodynamic phenomenon in which different particles respond in different ways to varying temperatures which has been studied by the Swiss chemist Charles Soret, has been difficult to examine in detail on Earth because of gravity. The SCOF (Soret-Facet) is the first investigation to verify Soret conditions in steady and changing conditions and was conducted in space. The objective of this study is to present a mathematical observation of a sample taken in a vertical channel formed by two infinite vertical parallel plates to study Soret effect as an alternative to expensive space experiments. It studies the heat transfer of a fluid in a channel with one moving relative to the other, driven by two different rates of diffusion and observes how different particles in that fluid respond to varying temperatures. The methods employed on the governing coupled-nonlinear momentum and energy equations obtained from Navier-Stokes equations are implicit finite difference using FORTRAN. Exact solutions from integration are obtained for steady state dimensionless velocity, concentration, temperature for a fully developed flow using MATLAB. It is observed that time, buoyancy ratio and thermophoretic coefficient increase velocity at hot plate. These results are applied to studies in mass transport with heat and energy, including those in the Earth's interior, oceans, atmosphere and in the refinement of crude oil. Conclusions are drawn from graphical representations of fluid velocity and fluid concentration for various parametric values.

Keywords:

Double diffusive Convection,
Couette flow,
Soret effects,
Navier-Stokes equations,
Parallel plates,
Boundary conditions.

INTRODUCTION

The Soret effect in fluids is a thermodynamic phenomenon in which different particles respond in different ways to varying temperatures. The effect, studied by the Swiss chemist Charles Soret, has been difficult to examine in detail on Earth because of gravity. The Study on Soret effect (thermal diffusion process) for the mixed solution by the in-situ observation technique facilitated at SCOF (Soret-Facet) is the first investigation to verify Soret conditions in steady and changing conditions, and to compare the Soret effect in microgravity with results on the ground, an important measurement for calibrating future investigations.

Migration of particles suspended in a gas can occur due to light, an electric field, temperature gradient or the gradient of vapor molecules. Thermophoresis is the event when particles suspended in a gaseous medium move away from a place of higher temperature and towards the place of lesser temperature. The force

responsible for pushing slow moving particles to the warmer region through the kinetically energized faster warmer particles is referred to as thermophoretic force. The thermophoretic transport can be of great use in thermal power plants, fossil power plants, textile industries, coal mines and coal-fired power plants for controlling pollution and the management of waste of (for example) unburned carbon emissions. Tsai & Lu (1995) studied deposition of particles using thermophoresis in a 2-plated parallel-walled channel of a precipitator. Mensch & Clearly (2019) provided measurements to an application in transport and filtration of specks of soot. Thermophoretic deposition and transport can be applied to biological flows in the transport of micro-organisms confined to channels as can be observed in Weiquan & Guoqian (2019). Experimental studies of thermophoretic deposition of soot particles from exhaust pipes of diesel engines was analysed by Messerer *et al.* (2003).

Brock (1962) presented a theory on thermophoretic force in the slip-flow regime. Modelling thermophoretic force depended on a ratio referred to as the Knudsen number $Kn = \lambda/D_p$, with D_p given as diameter of particle with mean free path λ of gaseous surrounding. A regime is a continuum regime if $Kn \ll 1$, slip-flow or transition if $Kn \sim 0.1$ and free-molecule if $Kn \gg 1$. According to a reassessment and clarification of modelling of spherical particles, Young (2011) analysed that Talbot *et al.* (1980) generalized the thermophoretic force coefficient for all regimes by considering Epstein-Stokes-Brock-Basset and Waldmann models of different regimes. Beresnev & Chernyak (1995) presented an approximation to the thermophoretic coefficient for an arbitrary Knudsen number by considering the Bhatnagar-Gross-Krook and Shakhov models of kinetic equation. Guha & Samanta (2014) compared the two models and concluded that the differences were negligible for $D_p < 100nm$.

Assuming a fluid is laminar and a fully developed forced convective flow with a pressure gradient and thermophoretic force, then Srinivasacharya *et al.* (2016) presents influences of variable properties along a wavy vertical plate inserted in a fluid saturated permeable medium. Grosan *et al.* (2009) and Magyari (2009) both studied thermophoretic transportation particles in fully developed mixed-convection flow in a parallel-plated vertical channel, in numerical and analytical solutions respectively. Shehzad *et al.* (2014) studied transfer of heat and mass in a three-dimensional Oldroyd-B fluid flow using Rosseland approximation. Zeeshan *et al.* (2014) observed activation energy and chemical reaction in a Couette-Poiseuille nanofluid flow. An analysis of a Couette- Poiseuille MHD nanofluid flow with Hall effects and radiation is investigated by Tlili *et al.* (2018) using Buongiorno model.

Heat and mass transfer usually have pressure force accompanied by buoyancy forces in some cases referred to as mixed convection. In parallel-plated vertical channels, the fluid flow may be upward i.e. in the direction of convection currents or downward i.e. pressure force is in opposite direction of convection currents. Large amount of studies considers upward flows with heating in one or both plates in a channel laden with aerosol particles with natural or mixed convections. Sasse *et al.* (1994) experimented on filtration of particles using thermophoresis in a free convective flow between parallel plates and also in tubes. The modelling of fluid flow in between parallel vertical plates as a result of mixed convection can be seen in Gradinger & Laneryd (2019). Olsson (2007) observed natural convection between parallel vertical plates. Sarveshanand & Singh (2015) investigated MHD natural convection between vertical porous plates. Gaur *et al.* (2018) studied unsteady natural convection flow with Radiation and heat generation in between parallel

vertical walls with a slip boundary condition and asymmetrical heating/cooling. Brereton & Mehravaran (2013) studied Sherwood numbers in a thermophoretic laminar flow depositing submicron-particles along a channel bounded by two walls.

Couette flow is a flow between horizontal or vertical parallel plates, where we have one plate stationary and the other moving with a velocity (in our case a velocity u_0). Narahari (2010) studied natural convection in between parallel vertical walls in an unsteady radiative Couette flow with a constant heat transfer rate. Boronin & Osiptsov (2020) investigated the stability of a Couette flow in a vertical channel of settling particles. By reducing governing equations into some modified Orr-Sommerfeld equation, a two-fluid approach taking into account two different particle number distribution in density.

Jha and Sani (2021) investigated unsteady and steady states of thermophoretic natural convection in a Couette fluid flow in a vertical channel of two parallel vertical plates. Jha (2001) studied an unsteady state of an MHD natural convection in a Couette flow. Owuor *et al.* (2020) studied a hydromagnetic Couette flow in a channel bounded by vertical semi-infinite porous walls. Das *et al.* (2014) observed the effects of suction and a heat generating radiation on a an unsteady free convective hydromagnetic Couette flow. Jha *et al.* (2020) presented a generalization of a transient Taylor-Couette fluid flow using semi-analytical methods of solution. Isah, Jha & Lin (2018) presented an analysis of a Couette flow of a fluid conducting electricity.

Experimental overview inside the Ryutai rack in the Japanese Experiment Module (JEM) aboard the International Space Station, (NASA, 2021) carried out experiments with a view to determine the:

Precise determination of the Soret coefficient which is not able to be performed on earth due to the experimental constraints that relate to the phenomenon of convection under gravity conditions.

This research focuses on observing Soret physics under steady, non-steady, and transient conditions- for comparisons with Soret effects with convection-controlled observations during experiments.

Results from the research improve scientists' understanding of thermodiffusion, a temperature-related effect in which different particles exhibit different behaviors in response to a temperature gradient. These results are applied to studies of mass transport, including heat and energy in Earth's interior, oceans and atmosphere. The investigation also applies to refinement of crude oil, crucial for transportation and many other uses on Earth. The paper aims to show the effect of temperature gradient in heat and mass transfer in a mixed convection flow using Robin thermal boundary conditions with a high Schmidt number. The Study aims to display the use of numerical methods in nonlinear

coupled equations and the use of boundary conditions that take into consideration insulation aspect.



Figure 1: NASA Image: ISS040E019216 - Photographic documentation of the installation of the Soret-Facet into the Solution Crystallization Observation Facility (SCOF) inside the Ryutai rack in the Japanese Experiment Module (JEM) aboard the International Space Station (ISS)

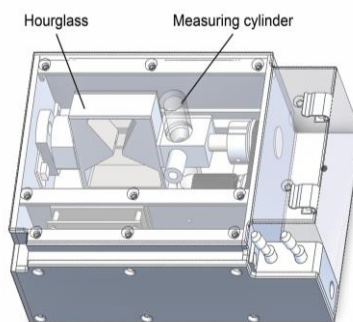


Figure 2: NASA Image: JSC2019E039831 - Schematic of Hourglass apparatus. Image courtesy of JAXA.

The objective of this study is to present a mathematical observation of a sample taken in a vertical channel formed by two infinite vertical parallel plates to study Soret effect as an alternative to expensive space experiments. The aim of this study is to present mathematical solutions to Soret effects with diffusion caused by two mechanisms in a Couette flow as analytic solutions and provide numerical analysis of transient mixed convective mass transfer flow in a vertical channel formed by two infinite vertical parallel plate in the presence of thermophoresis of a viscous incompressible fluid.

Mathematical Modelling as an Alternative

We present a thermophoretic fully developed regime that is also time-dependent, unsteady and a free convective Couette flow in a vertical channel formed by two parallel walls of negligible thickness. As seen in Fig.1a., we let x' - axis be along vertical length of channel walls and y' - axis be across channel in the horizontal. Let the walls at $y' = 0$ and $y' = L$ be parted by a distance L .

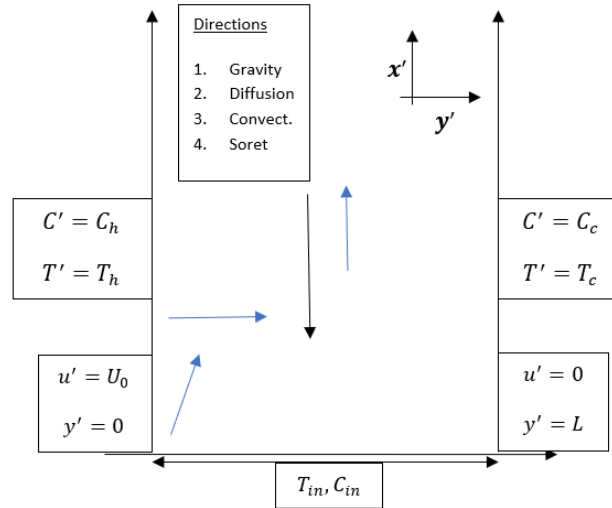


Figure 3a: The model in geometrical form



Figure 3b: Particle deposition at the corner of a room

Initially i.e. at $(t' \leq 0)$, both walls have velocity zero, temperature of the fluid and two walls are taken as T_0 . At a time afterwards, $(t' > 0)$, the plate at $y' = 0$ starts moving momentarily along the x' - axis with a velocity U_0 , while plate at $y' = L$ remains at rest; temperature of the channel wall at $y' = 0$ changes from T_0 to T_h , and the temperature of the wall at $y' = L$ becomes T_c . We have $T_h > T_c$ which causes thermophoretic and natural convection flow. Let the concentration at hot wall (at $y' = 0$) be assumed to be C_h and that of the cold wall be C_c . If $T' = T'(y', t')$, $C' = C'(y', t')$, $u' = u'(y', t')$ and the velocity vector $\mathbf{v} = (u', v')$. We assume the fully developed regime relations of $v' = 0$, $\frac{\partial v'}{\partial y'} = 0$, $\frac{\partial p}{\partial y'} = 0$.

Under the usual Boussinesq approximation, the difference in temperature across channel $\Delta T = T_h - T_c$. The characteristic temperature and Concentration are $T_0 = (T_h + T_c)/2$ and $C_0 = (C_h + C_c)/2$ respectively.

We take the characteristic density ρ_0 at temperature T_0 , $\nu := \mu/\rho_0$ is kinematic viscosity. Taking $\beta = -(1/\rho_0)(\rho - \rho_0/T - T_0)_{C,p=const.}$ and $\beta^* = -(1/\rho_0)(\rho - \rho_0/C - C_0)_{T,p=const.}$ as the coefficients of heat expansion and concentration expansion respectively. The following equations describe the current problem:

$$\frac{\partial u'}{\partial t'} = g\beta(T' - T_0) + g\beta^*(C' - C_0) + \nu \frac{\partial^2 u'}{\partial y'^2} - \frac{1}{\rho_0} \frac{\partial p}{\partial x} \tag{1}$$

$$\frac{\partial T'}{\partial t'} = \sigma \frac{\partial^2 T'}{\partial y'^2} \tag{2}$$

$$\frac{\partial C'}{\partial t'} = D \frac{\partial^2 C'}{\partial y'^2} - \frac{\partial}{\partial y'} (v_T C') \tag{3}$$

with $\sigma = k_f/c_p\mu$ is the thermal diffusivity. Define the

Brownian diffusivity $= \frac{\kappa T' C_c}{3\pi\mu D_p}$. Let k_f be the thermal conductivity of wall. The initial and boundary conditions to the above equations are:

$$t' \leq 0 : u' = 0, T' = T_0, C' = 0 \text{ for } 0 \leq y' \leq L$$

$$t' > 0 : \begin{cases} u' = U_0, T' = T_h, (1 - B)C' + B \frac{dC'}{dy'} = (1 - B)C_h - B \frac{D'}{D} \left[C_0(1 - C_0) \frac{dT'}{dy'} \right] & \text{at } y' = 0 \\ u' = 0, T' = T_c, (1 - B)C' + B \frac{dC'}{dy'} = (1 - B)C_c - B \frac{D'}{D} \left[C_0(1 - C_0) \frac{dT'}{dy'} \right] & \text{at } y' = L \end{cases} \quad (4)$$

where $\Delta C = -C_0(1 - C_0) \frac{D'}{D} \Delta T'$ (5)

stands for Soret-Driven Convection

Describing the volumetric flow rate

$$Q = \int_0^L u' dy \quad (6)$$

Thermophoretic depositional speed with direction along the y' -axis, v_T is written as:

$$v_T = -k \frac{v}{T'} \frac{\partial T'}{\partial y'} \quad (7)$$

where k in this case is the thermophoretic force coefficient in dimensional form. Let k be defined by Beresnev and Chernyak (1995) based on the Bhatnagar-Gross-Krook and Shakhov model that considers particle-reflection of colliding molecules:

$$k = \frac{\pi}{Kn} \mu v r \left[\frac{\lambda_r f_{11} + f_{21}}{\lambda_r f_{31} + (\lambda_r + 5Kn) f_{41}} \right] \quad (8)$$

If the accommodation factor for energy equals that of momentum which equates to one, then for the transition regime i.e., $0.05 < Kn < 5$, the values of coefficients f_{11} , f_{21} , f_{31} and f_{41} are provided in a table in Beresnev and Chernyak (1995) for various values of Knudsen number by taking ratio $\lambda_r \equiv k_f/k_p$.

Introducing the following dimensionless quantities in equation (1) – (3)

$$y = \frac{y'}{L}, u = \frac{u'}{U_0}, Gr = \frac{g\beta L^3(T_h - T_c)}{v^2}, \theta = \frac{T' - T_0}{T_h - T_c}, \phi = \frac{C' - C_0}{C_h - C_c}, Pr = \frac{\nu}{\alpha}, Sc = \frac{\nu}{D}, t = \frac{t'v}{L^2}, b = \frac{\beta^*(C_h - C_c)}{\beta(T_h - T_c)}, N_t = \frac{T_0}{T_h - T_c}, N_c = \frac{C_0}{C_h - C_c}, Q = U_0 L, a_T = \frac{T_0 - T_2}{T_{in} - T_0}, a_c = \frac{C_0 - C_2}{C_{in} - C_0}, V_T = \frac{L}{v} v_T \quad (9)$$

equation (7) can be written in the dimensionless form as:

$$V_T = - \frac{k}{(\theta + N_t)} \frac{d\theta}{dy} \quad (10)$$

If $\alpha = \frac{L^2}{u_0 \mu} \frac{\partial p}{\partial x}$ is the dimensionless pressure gradient along the x –direction then, dimensionless momentum, energy and concentration equations are:

$$\frac{\partial u}{\partial t} = \frac{\partial^2 u}{\partial y^2} + \frac{Gr}{Re} [\theta + b\phi] - \alpha \quad (11)$$

$$\frac{\partial \theta}{\partial t} = \frac{1}{Pr} \frac{\partial^2 \theta}{\partial y^2} \quad (12)$$

$$\frac{\partial \phi}{\partial t} = \frac{1}{Sc} \frac{\partial^2 \phi}{\partial y^2} + k \frac{\partial}{\partial y} \left[\frac{\phi + N_c}{\theta + N_t} \frac{\partial \theta}{\partial y} \right] \quad (13)$$

the initial and boundary conditions in dimensionless form become:

$$t \leq 0 : u = 0, \theta = 0, \phi = 0 \text{ for } 0 \leq y \leq 1$$

$t > 0$:

$$\begin{cases} u = 1, T' = a_T, (1 - B)\phi + B \frac{d\phi}{dy} = (1 - B)a_c - B \frac{d\theta}{dy} & \text{at } y' = 0 \\ u = 0, T' = -a_T, (1 - B)\phi' + B \frac{d\phi}{dy} = -(1 - B)a_c - B \frac{d\theta}{dy} & \text{at } y' = 1 \end{cases}$$

in dimensionless form the

$$\int_0^1 u dy = 1 \quad (14)$$

Analytical Solutions

Presenting the governing equations in a steady state will produce closed-form solutions to the problem illustrated in Fig. 1. and modelled above. The equations (11) - (14) in steady state with their relevant boundary conditions in this case are:

$$\frac{\partial^2 u}{\partial y^2} + \lambda(\theta + b\phi) - \alpha = 0 \quad (15)$$

$$\frac{\partial^2 \theta}{\partial y^2} = 0 \quad (16)$$

$$\frac{\partial^2 \phi}{\partial y^2} + kSc \frac{\partial}{\partial y} \left(\frac{\phi + N_c}{\theta + N_t} \frac{\partial \theta}{\partial y} \right) = 0 \quad (17)$$

The boundary conditions (14)

Case i: when $B = 0$

Corresponds to double-diffusive convection for which the solutal buoyancy forces are induced by the imposition of a constant concentration such as $\phi = a_c$ on $y = 0$ and $\phi = -a_c$ on $y = 1$

Case ii: a binary fluid subject to the the Soret effect.

The boundary conditions will be

$$\frac{d\phi}{dy} = \frac{d\theta}{dy} \quad (18)$$

We solve for Case i) by letting $a = kSc$ and $z = N_t + \frac{1}{2} - y$. The solutions for the energy, concentration and momentum equations are given as

$$\theta = \frac{1}{2} - y \quad (19)$$

$$\phi = -\frac{1}{(1+a)}K_1z + K_2z^{-a} - N_c \quad (20)$$

$$u = -\lambda \left[\frac{b_2z^3}{6} - \frac{b_1z^2}{2} + \frac{b_3z^{2-a}}{(1-a)(2-a)} \right] + \alpha \frac{z^2}{2} + K_3z + K_4 \quad (21)$$

where $K_1 \dots K_4$ are all constants given in the Appendix

Numerical Solutions

Equations (11)-(13) are made discrete by finite difference Scheme. If $Sc \neq 0$ and $Pr \neq 0$, in order to approximate the initial-boundary value problem, we introduce a rectangular mesh of points $(i\Delta y, j\Delta t)$ in the channel $[0,1]$ with $0 = y_0 < y_1 < \dots < y_n = 1$ and $0 = t_0 < t_1 < t_2 < \dots$ and having a uniform mesh along both axes of $\Delta y = y_{i+1} - y_i$ and $\Delta t = t_{j+1} - t_j = \frac{1}{N}$. Separating into groups of J intervals of equal size at t values labeled $j = 0, 1, \dots, J$ also $[0,1]$ dividing the interval into I intervals spaced equally at y values labeled $i = 0, 1, \dots, I$.

We call on the Thomas algorithm to invert the tridiagonal matrices in FORTRAN. These processes continue until a steady state value is reached that observes the convergence criterion $\frac{\sum |A_{i,j+1} - A_{i,j}|}{(I-1)|A|_{max}} < 10^{-5}$ is achieved.

RESULTS AND DISCUSSION

In this study, aerosol Schmidt number is assumed as $(\geq 10^3)$ consistent with Tsai & Lin (1999) therefore $Sc = 1000$ is used throughout the profiles for aerosol particles $0.01\mu m \leq D_p \leq 10\mu m$ usually having

Schmidt number from 2.87×10^2 to 6.20×10^6 according to Friedlander (1977). Effects of pressure gradient is considered at a) no pressure b) negative pressure gradient and c) adverse pressure gradient. Increasing the fluid pressure is akin to increasing the potential energy of the fluid and hence reducing the kinetic energy and a deceleration of the fluid. The mixed convection parameter is considered either as the Richardson number Ri or as a buoyancy parameter λ . In this study, $\lambda = 1.0$ represents typical mixed convection flow, $\lambda = -100$ represents a forced convection dominated flow and $\lambda = 100$ represents a natural convection dominated flow. The ratios of thermophoresis, concentration and buoyancy N_t, N_c, b , are varied. Variations in the Richardson number are compared at $Re = 90$ and $Re = 900$.

Velocity Profiles

Figures 2(a), 2(b) and 2(c) below display graphs of velocity when natural convection dominates the flow. They show effects of thermophoresis and pressure gradient on transient and steady state velocity. Figure 2(d) below show a typical mixed convection flow ($\lambda = 1$) where the influences of forced and natural convection are equal on flow for $\alpha = 0, \alpha = 100, \alpha = 10, \alpha = -10$ and $\alpha = -100$ respectively.

2(e) display the effect of negative pressure gradient on a thermophoretic typically mixed convective flow. It can be observed that velocity is positive with positive pressure gradient and negative with negative pressure gradient. Reduction in pressure gradient from $\alpha = 100$ to $\alpha = 10$ moves minimum values to maximum values. At $\alpha = -10$ with increase in time, velocity changes from having a minimum value to having a maximum value. At $\alpha = -100$, with increase in time, velocity profiles have an additional increase to their maximum values. Figure 2(f) depicts velocity profiles for different flow of aerosol particles of different diameters, it is observed that at $Sc = 10^3$ and $Sc = 10^4$ velocities concede. Increase in Schmidt number improves velocity. Figure 2(g) shows that increase in the buoyancy ratio increases velocity.

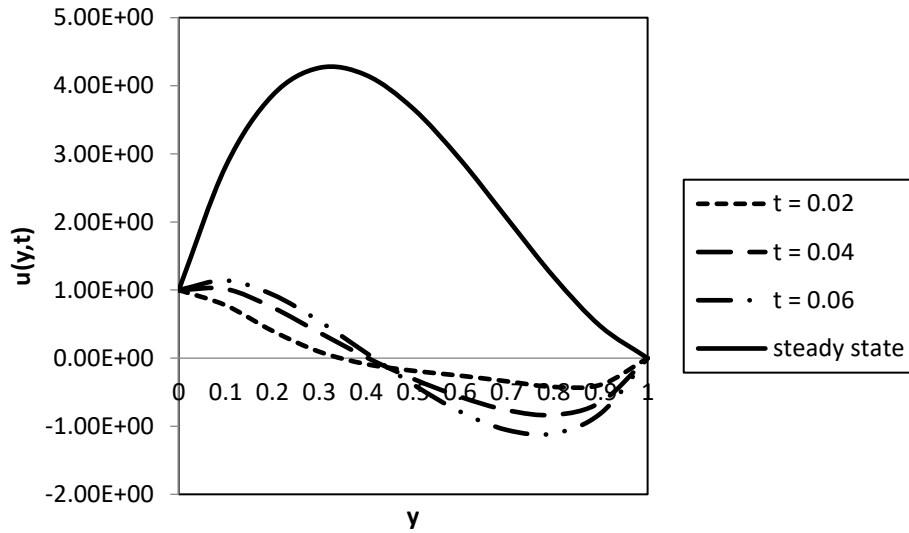


Figure 4a: Velocity profile for aiding flow
 ($k = 1.2, Pr = 0.71, Sc = 1000, b = 1.0, N_c = 2.0, N_t = 8.0, \alpha = 10, \lambda = 100$)

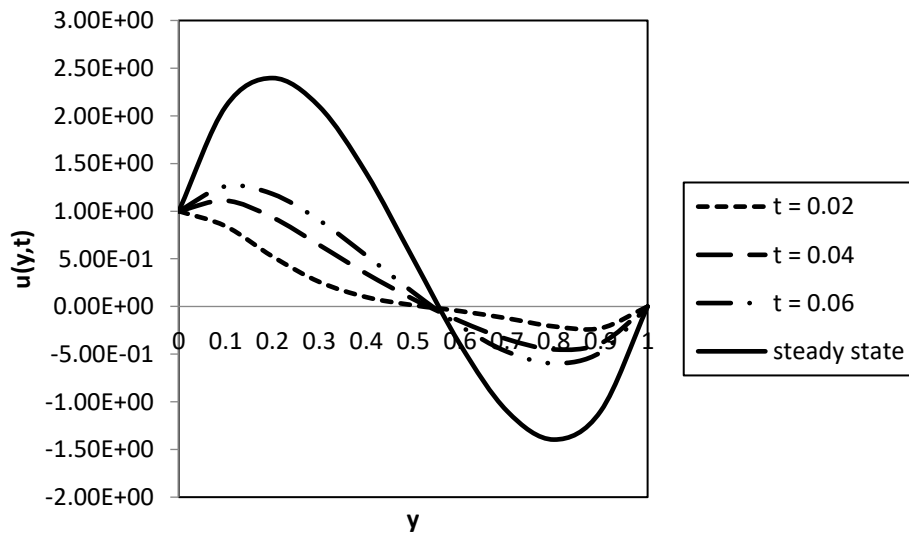


Figure 4b: Velocity profile for aiding flow, no pressure gradient
 ($k = 0, Pr = 0.71, Sc = 1000, b = 1.0, N_c = 2.0, N_t = 8.0, \alpha = 0, \lambda = 100$)

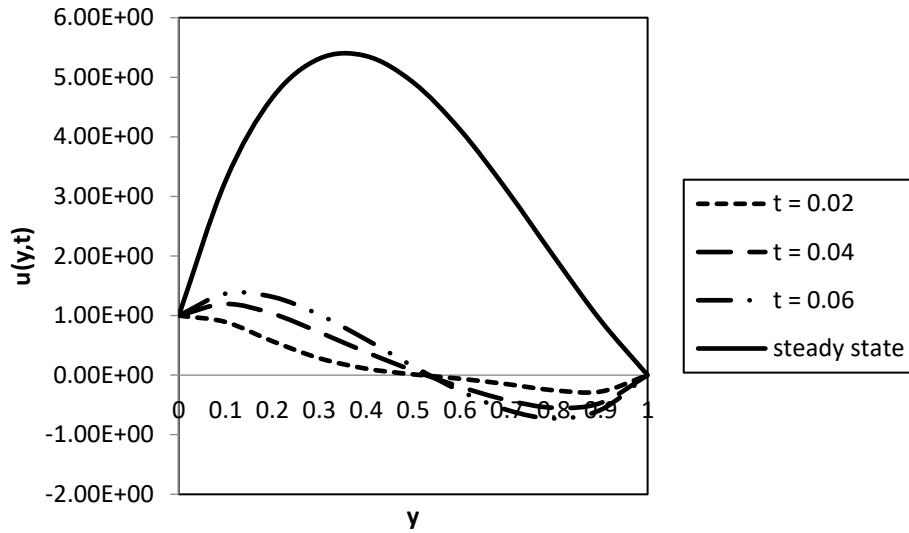


Figure 4c: Velocity profile for opposing flow, no pressure gradient
 ($k = 1.2, Pr = 0.71, Sc = 1000, b = 1.0, N_c = 2.0, N_t = 8.0, \alpha = 0, \lambda = 100$)

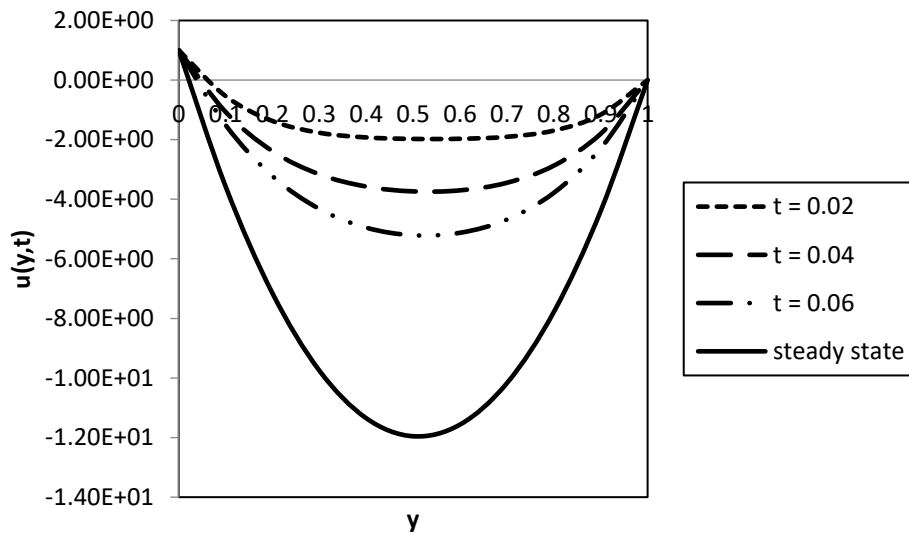


Figure 4d: Velocity profile for equal influence of forced and natural flow ($k = 1.2, Pr = 0.71, Sc = 1000, b = 1.0, N_c = 2.0, N_t = 8.0, \alpha = 100, \lambda = 1$)

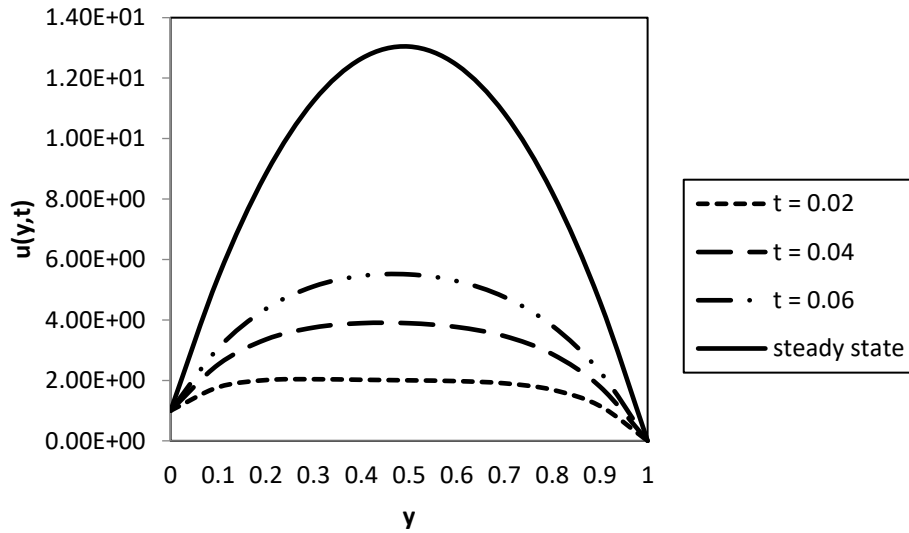


Figure 4e: Velocity profile for equal influence of forced and natural flow ($k = 1.2, Pr = 0.71, Sc = 1000, b = 1.0, N_c = 2.0, N_t = 8.0, \alpha = -100, \lambda = 1$)

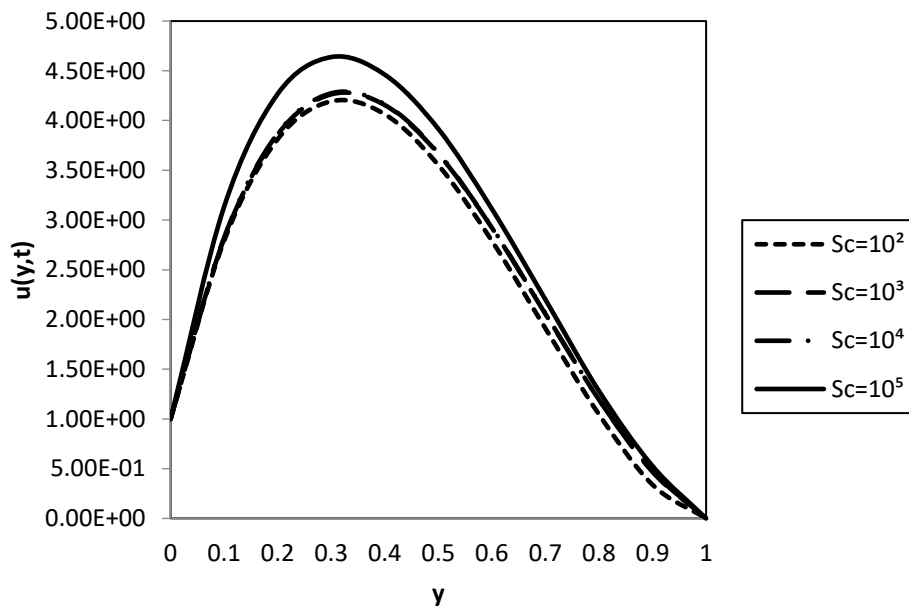


Figure 4f: Velocity profile for variations in Schmidt number for equal influence of forced and natural flow ($k = 1.2, Pr = 0.71, t = 5, b = 1.0, N_c = 2.0, N_t = 8.0, \alpha = 10, \lambda = 100$)

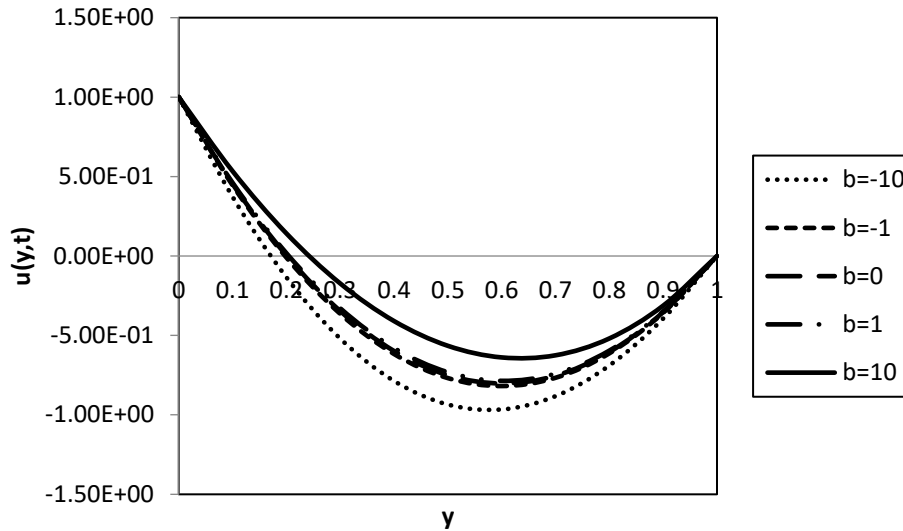


Figure 4g: Velocity profile with variations in the buoyancy ratio ($k = 1.2, Pr = 0.71, Sc = 1000, b = 1.0, N_t = 8.0, t = 5, \alpha = 10, \lambda = 0.5$)

Particle Concentration Profiles

Figure 3(a) shows a symmetrical concentration profile passing through the centreline. In the absence of thermophoresis i.e. $k = 0$; $Pr = 0.71, Sc = 1000, N_c = 2.0, N_t = 8.0$ for $t = 2, 4, 6$ and steady state concentration. It is observed that from about $y = 0.3$ to $y = 0.7$, concentration is zero. Figures 3(a) and 3(b) displays the drastic change in aerosol particle concentration from zero thermophoresis to $k = 1.2$. Figure 3(c) displays symmetrical concentration profile passing through the channel centre for different values of the Schmidt number $Sc = 0.25, 10, 15, 100$. It is observed that there is a huge increment in particle

concentration from $Sc = 10$ to $Sc = 15$ and a relatively small increment in concentration from $Sc = 15$ to $Sc = 100$. Concentration at $Sc = 0.25$ is linear while at $Sc = 100$ (is interesting) at $y = 0.12$ and $y = 0.8$. Figures 3(a) shows that with increase in time comes increase in concentration at transient and steady states. Figures 3(a) and 3(b) show that thermophoresis greatly disturbs the distribution of concentration level across the channel in a flow of aerosol particles in air which is consistent with Sasse *et al.* (1994). Figure 3(c) displays the effect of Schmidt number on concentration: increase in Schmidt number reduces concentration of particles.

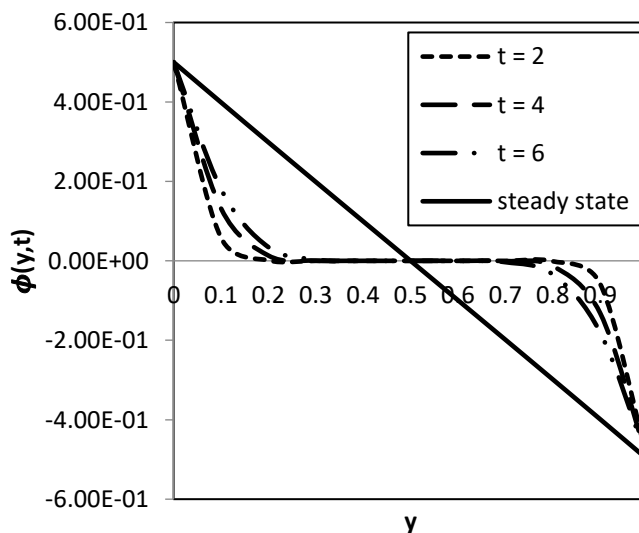


Figure 5a: Concentration profile for ($k = 0, Pr = 0.71, Sc = 1000, N_c = 2.0, N_t = 8.0$)

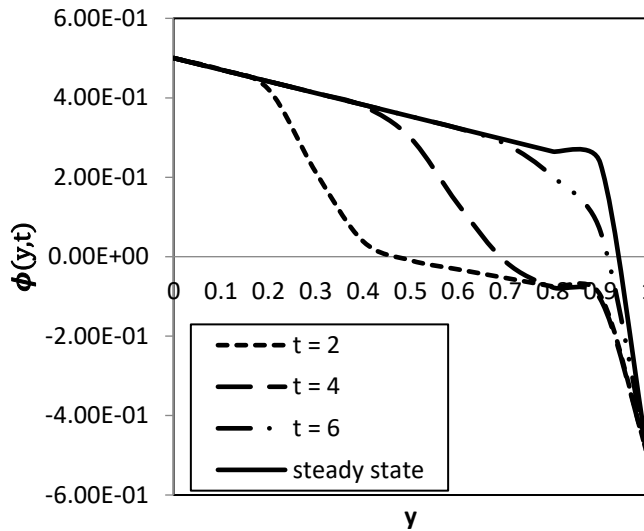


Figure 5b: Concentration profile for $(k = 1.2, Pr = 0.71, Sc = 1000, N_c = 2.0, N_t = 8.0)$

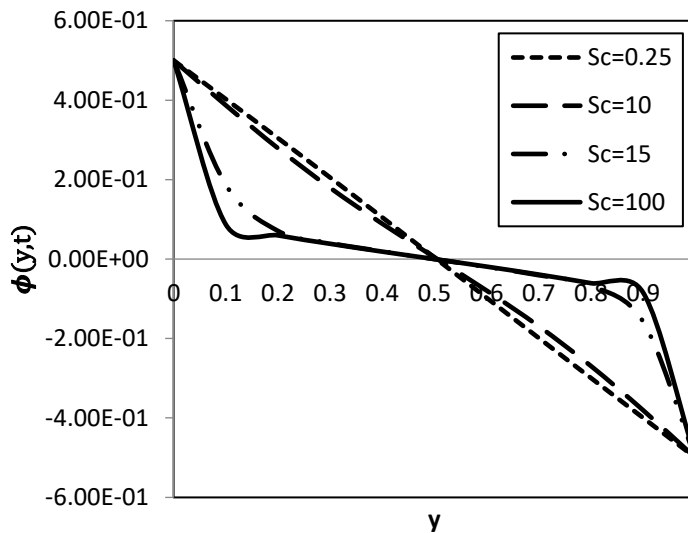


Figure 5c: Concentration profile for different values of the Schmidt number $(k = 1.2, Pr = 0.71, t = 0.05, N_c = 2.0, N_t = 8.0)$

CONCLUSION

Numerical as well as analytical solutions are derived for transient and steady mixed convective and mass transfer Couette flow in vertical channel formed by two infinite vertical parallel plates in the presence of thermophoresis. The temperature, velocity and concentration fields are obtained in closed form for the steady mixed convection Couette flow in a vertical channel while the transient states are obtained numerically by implicit finite difference technique.

Graphical results show effects of pressure gradient considered at a) no pressure b) negative pressure gradient and c) adverse pressure gradient of aerosol particles represented with $Sc = 1000$. These graphs reveal that in the presence of thermophoresis, when pressure gradient α is increased from 0 to a positive value, velocity moves from positive to negative values for both transient and steady states ; increase in Schmidt number improves velocity; velocity increases with increase in thermophoretic parameter N_t until $N_t = 6.0$

is reached; velocity decreases monotonically with increase in concentration ratio N_c ; velocity is independent of the Reynolds number Re ; increase in the buoyancy ratio increases velocity; increase in time increases concentration at transient and steady states; thermophoresis greatly disturbs the distribution of concentration level across the channel in a flow of aerosol particles in air; the parameter $a = kSc$ is more effective than the parameter k in improving concentration levels across the channel; increase in Schmidt number reduces concentration of particles. This mathematical modelling provides alternatives to experiments conducted under difficult and expensive, steady, non-steady and transient conditions and also suggests data generating models for comparisons in studies of Soret effects with convection-controlled observations during experiments.

REFERENCES

Batchelor G.K. & Shen C. (1985). Thermophoretic deposition of particles in gas flowing over cold surfaces, *J. Colloid Interface Sci.*, 107 (1), 21-37.

Beresnev, S. & Chernyak, V. (1995). Thermophoresis of a spherical particle in a rarefied gas: numerical analysis based on the model kinetic equations. *Physics of fluids*. 7, 1743-1756.

Boronin, S.A. & Osipov, A. N. (2020). Stability of a vertical Couette flow in the presence of settling particles. *Physics of fluids*. 32, 024104.

Brereton, G. J. & Mehrvaran, M., A. (2013). Thermophoretic Sherwood number for characterizing submicron-particle mass transfer in laminar wall-bounded flows, *Aerosol Sci. Tech.* 47 (6) 123-133.

Brock, J. R. (1962). On the theory of thermal forces acting on aerosol particles. *J. Colloid Sci.* 17, 768-780.

Das, S. S., Panda, S. & Bera, N. C. (2014). Hydromagnetic convective Couette flow in presence of time dependent suction and radiative heat source, *Int. J. Eng. and Appl. Sci.* 1(3) 1123.

Friedlander S. K. (1977). Smoke, Dust, Haze: Fundamentals of Aerosol Behavior. Wiley. New York, 32.

Gaur, P. K., Sharma, R.P. & Jha, A. K. (2018). Transient free convective Radiative flow between vertical parallel plates heated/cooled asymmetrically with heat generation and slip condition. *Int. J. Appl. Mech. and Eng.*, 23 (2), 365-385.

Gradinger, T. B. & Laneryd, T. (2019). Modelling of mixed convection between vertical parallel plates in electric equipment immersed in high Pr liquids. *J. thermal Sci. Eng. Appl.* 11 (5), 051005.

Grosan, T., Pop, R. & Pop, I. (2009). Thermophoretic deposition of particles in fully developed mixed convection flow in a parallel-plate vertical channel. *Heat Mass Transf.* 45, 503-509.

Guha, A. & Samanta, S. (2014). Effect of thermophoresis and its mathematical models on the transport and deposition of aerosol particles in natural convective flow on vertical and horizontal plates. *J. Aerosol Sci.* 77, 85-101.

Isah, B. Y., Jha, B.K. & Lin, J.-E. (2018). On Couette flow of conducting fluid, *Int. J. Theoretical and Appl. Math.*, 4(1), 8-21.

Jha, B. K. & Sani, H. N. (2021). Thermophoresis on free convective unsteady/steady Couette fluid flow with mass transfer. *Int. J. Appl. Comp. Math.* 7 (80). DOI:10.1007/540819-021-00980-0

Jha, B. K. (2001). Natural Convection in unsteady MHD Couette flow. *Heat and Mass Transfer*. 37, 329-331.

Jha, B. K. & Danjuma, Y. K. (2020). Transient generalized Taylor-Couette: A semi-analytical approach. *J. Taibah Uni. Sci.* 14 (1), 445-453.

Langtangen, H. P. (2003). *Computational Partial Difference equations: Numerical methods and Diffpack programming*. Springer. 459-491.

Magyari, E. (2009). Thermophoretic deposition of particles in fully developed mixed convection flow in a parallel-plate vertical channel. *Heat Mass Transf.* 45, 1473-1482.

Mensch, A. E. & Clearly, G. T. (2019). Measurements and Predictions of thermophoretic soot deposition. *Int. J. Heat Mass Transf.* 143 (10), 1016.

Messerer, A., Niessner, R. & Pöschl, U. (2003). Thermophoretic deposition of soot aerosol particles under experimental conditions relevant for modern diesel engine exhaust gas systems, *J. Aerosol Sci.* 34 (8), 1009-1021.

Narahari, M. (2010). Effect of thermal Radiation and Free convection on the unsteady Couette flow between two vertical parallel plates with constant heat flux at one boundary. *WSEAS Trans. Heat and Mass Transfer*. 5, 21-30.

Olsson, C.-O. (2007). *Buoyancy driven flow between vertical parallel plates of finite width*. Paper presented at the ASME/JSME 2007 Thermal Engineering Heat Transfer Summer Conference, Vancouver, British Columbia, Canada, 8-12 July 2007, 977-983.

Owuor, O.C., Kinyanjui, M.N. & Kiogora, P.R. (2020). Hydromagnetic Couette flow between two vertical semi-infinite permeable plates. *Int. J. Advances Appl Math and Mech.* 7(4), 1-13.

Sarveshanand & Singh, A. K. (2015). Magneto hydrodynamic free convection between vertical porous plates in the presence of induced magnetic field. *Springerplus.* 333 (2015).

Sasse, A. G. B. M., Nazaroff, W. W. & Gadgil, A. J. (1994). Particle filter based on thermophoretic deposition from natural convection flow. *Aerosol Sci. Tech.* 20 (3), 227- 238.

Shehzad A., Alsaedi, A., Hayat T. & Alhuthali M. S. (2014). Thermophoresis particle deposition in mixed convection three-dimensional radiative flow of an Oldroyd-B fluid, *J. of the Taiwan Inst. Chem. Eng.* 45(3), 787-794.

Srinivasacharya, D., Mallikarjuna, B. & Bhuvanavijaya, R. (2016). Effects of thermophoresis and variable properties on mixed convection along a vertical wavy surface in a fluid saturated porous medium. *Alexandria Eng Journal.* 55(2), 1243-1253.

Talbot, L., Cheng, R.K., Schefer, R.W. & Willis, D.R. (1980). Thermophoresis of particles in a heated boundary layer. *J. Fluid Mech.* 101 (4), 737-758.

Tlili, I., & Namadneh, N.N. (2018). Thermodynamic analysis of MHD Couette-Poiseuille flow of water-based nanofluids in a rotating channel with radiation and Hall currents. *J. of Thermal Analysis and Calorimetry.* 132, 1899-1912.

Tsai, C.-J. & Lu, H.-C. (1995). Design and Evaluation of a plate-to-plate thermophoretic precipitator. *Aerosol Sci. and Tech.* 22(2), 172-180.

Tsai R. & Lin Z. Y. (1999). An approach for evaluating aerosol particle deposition from a natural convection flow onto a vertical flat plate. *J. Hazardous Materials.* B 69, 217-227.

Weiquan, J., & Chen, G. (2019). Dispersion of active particles in confined unidirectional flows, *J. Fluid Mech.* 877 (25), 1-34.

Young, J. B. (2011). Thermophoresis of a spherical particle: Reassessment, Clarification, and New Analysis. *Aerosol Sci. and Tech.* 45 (8), 927-948.

Zeeshan, A., Shehzad, N. & Ellahi, R. (2018). Analysis of activation energy in Couette-Poiseuille flow of nanofluid in the presence of chemical reaction and convective boundary conditions. *Results in Physics.* 8, 502-512.

APPENDIX

$$a = kSc, b_1 = N_t + bN_c, b_2 = 1 - \frac{1}{(1+a)}K_1 \text{ and } b_3 = K_2 b$$

$$K_1 = -\frac{1}{2}(a+1) \left[\frac{(z_0)^{\alpha(1+2N_c)} - (z_1)^{\alpha(2N_c-1)}}{(z_0)^{\alpha+1} - (z_1)^{\alpha+1}} \right]$$

$$K_2 = \frac{(z_1)^{\alpha}(z_0)^{\alpha(N_t-N_c)}}{(z_1)^{\alpha+1} - (z_0)^{\alpha+1}}$$

$$K_3 = 1 + \frac{1}{2}[\alpha + \lambda b_1][z_1^2 - z_0^2] + \frac{b_2 \lambda}{6}[z_0^3 - z_1^3] + \frac{b_3 \lambda}{(1-a)(2-a)}[z_0^{2-a} - z_1^{2-a}]$$

$$K_4 = \left[\frac{1}{2} - N_t \right] + \frac{1}{2}[\alpha + \lambda b_1][z_1 z_0^2 - z_0 z_1^2] + \frac{b_2 \lambda}{6}[z_0 z_1^3 - z_1 z_0^3] + \frac{b_3 \lambda}{(1-a)(2-a)}[z_0 z_1^{2-a} - z_1 z_0^{2-a}]$$